Old Dominion University
ODU Digital Commons

OEAS Faculty Publications

Ocean, Earth & Atmospheric Sciences

1985

Fault Movements and Tectonics of Eastern Iran: Boundaries of the Lut Plate

Ali A. Nowroozi
Old Dominion University

A. Mohajer-Ashjai

Follow this and additional works at: https://digitalcommons.odu.edu/oeas_fac_pubs

Part of the Geochemistry Commons, Geophysics and Seismology Commons, and the Tectonics and Structure Commons

Fault movements and tectonics of eastern Iran: boundaries of the Lut plate

Ali A. Nowroozi *Department of Geological Sciences, Old Dominion University, Norfolk, Virginia 23508, USA*

A. Mohajer-Ashjai *Atomic Energy Organization of Iran, Tehran, Iran*

Summary. From 1977 March 21 to 1981 July 28, about 15 earthquakes with $M_s \geqslant 6.0$ and many earthquakes with $M_s \geqslant 4.5$ have occurred in Iran. The upsurge of seismic activity started following the Khorqu earthquake of 1977 March 21, $M_s = 7.0$, south-east of the Fars folded series of Zagros. This shock had a thrust focal mechanism solution indicating the general northward movement of the Arabian plate with respect to the Iranian landmass. It was followed by six major damaging earthquakes in eastern Iran. The earthquakes are associated with extensive faulting which surrounds the Lut plate. (1) The Zarand earthquake of 1977 December, $M_s = 5.8$, was associated with about 20 km of fault trace, severe mass wasting and about 20 cm of right lateral movement. (2) The Tabas earthquake of 1978 September, $M_s = 7.7$, with about 75 km of multiple thrust faulting and a maximum vertical displacement of 35 cm. (3) The Kurizan earthquake of 1979 November, $M_s = 6.0$, with more than 17 km of strike-slip fault trace and a maximum right-lateral displacement of 90 cm and a vertical displacement of 60 cm. (4) The Koli earthquake of 1979 November, $M_s = 7.1$, with at least 65 km of fault trace and a maximum left-lateral displacement of 255 cm and a vertical displacement of 380 cm. (5) Golbaf earthquakes of 1981 June, $M_s = 6.0$ with at least 16 km of observed fault trace and a maximum vertical displacement of 15 cm. (6) The Chaharfarsang-Sirch earthquake of 1981 July, $M_s = 7.1$, with about 70 km of discontinuous fault trace and 20 cm of right-lateral motion and 15 cm of vertical motion. Portable networks of seismographic stations were deployed following each event. Results of aftershock studies are compared with field observations. The observed faults and aftershock zones appear to mark the broad deformational boundaries of the Lut plate.

Key words: eastern Iranian tectonics, fault movements, Lut plate.

Introduction

Iran is one of the most seismically active countries in the world. The seismicity of Iran is discussed by Nowroozi (1971, 1976), Nabavi (1977), Berberian (1976), Shoja-Taheri & Niazi (1981), and
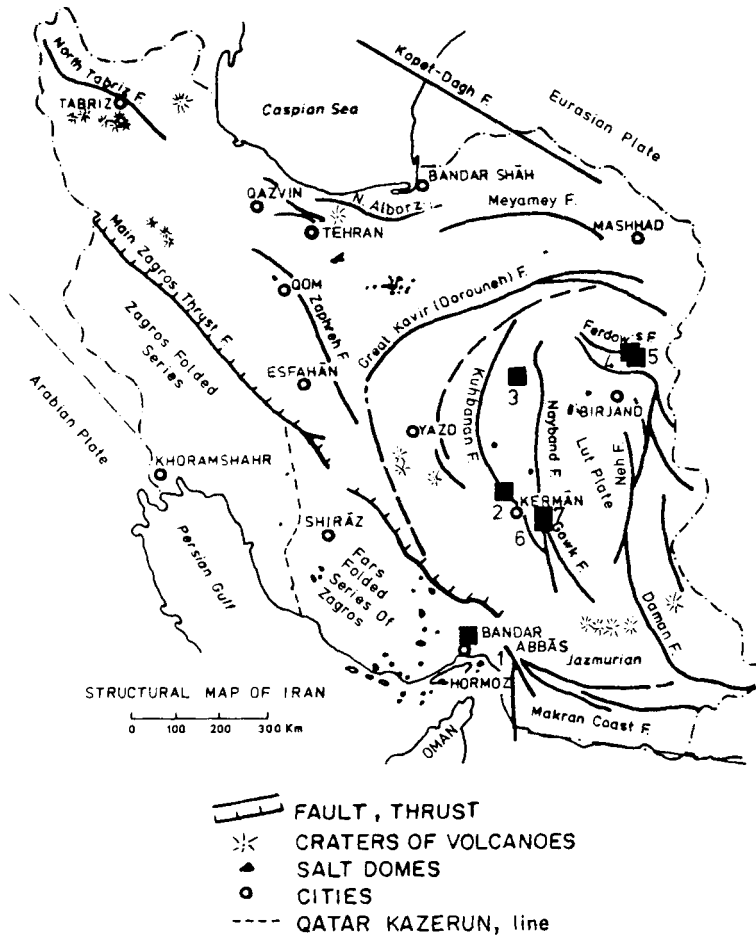
Figure 1. Locations of earthquakes discussed in this work. 1 – the Khorgu earthquake of 1977 March 21, M_s=7.0, seems to have started a period of intense seismicity. This event has a thrust focal mechanism indicating relative northward motion of the Arabian plate with respect to the Iranian land mass. Following this event, six earthquakes numbered 2 to 7 have occurred which are associated with extensive faulting. The faults mark part of the Lut plate.

Ambraseys & Melville (1982). Detailed field investigation after earthquakes for the purpose of mapping the fault traces and recording the aftershock activities are reported by a number of authors. A summary on these works prior to 1976 can be found in Berberian (1976). In this paper we will discuss the results of field investigations and aftershocks recording following occurrences of seven destructive earthquakes from 1977 to 1981 in eastern Iran. In contrast to the Zagros regions where, as a rule no apparent surface fault trace is observable following even a large earthquake, in eastern Iran earthquakes are often associated with well recognizable surface faulting. The locations of these events are numbered in Fig. 1, and their parameters are given in Table 1.

Portable networks of seismographic stations were deployed following each earthquake, and the HYPOELLIPSE computer program (Lahr & Ward 1973) was used for locating the seismic events. The regional crustal structures are not well known in this area, thus various models are considered and a model which produced the least time residual and scatter in epicentral position was used.

Table 1. Source parameters of earthquakes.

Event no.	Date	Origin time	Latitude, °N	Longitude, °E	Depth, km	M_S	Source name
1	1977 Mar. 21	21:18:54.6	27.69	56.49	33	7.0	Khorgu, Zagros folded belt
2	1977 Dec. 19	23:34:26.6	30.90	56.66	10	5.8	Zarand, Kuh-Banan fault
3	1978 Sept. 16	15:35:52	33.40	57.34	10	7.7	Tabas; Tabas fault
4	1979 Nov. 10	01:21:22.1	33.92	59.74	35	6.6	Kurizan fault
5	1979 Nov. 27	17:10:32.9	33.96	59.73	10	7.1	Koli fault
6	1981 June 11	07:24:25.2	29.91	57.72	33	6.8	Gowk fault
7	1981 July 28	17:22:24.6	30.01	57.79	10	7.1	Gowk Lakar-Kuh fault

Based on azimuthal distribution of stations and travel-time residual, locations were graded. The reported events in this paper have a grade of A to D, and their positions may be off from 2 to 7 km.

The seismic data and faultings are interpreted in terms of a smaller Lut plate surrounded by several broad zones of deformations. The inner limit of this plate and the outer deformational zones are discussed.

The Khorgu Earthquake of 1977 March 21

The Khorgu earthquake occurred in the Fars folded series of Zagros (Nowroozi 1976), about 60 km north of the Bandar-e-Abbas. Berberian & Papastamatiou (1978) reported on damage
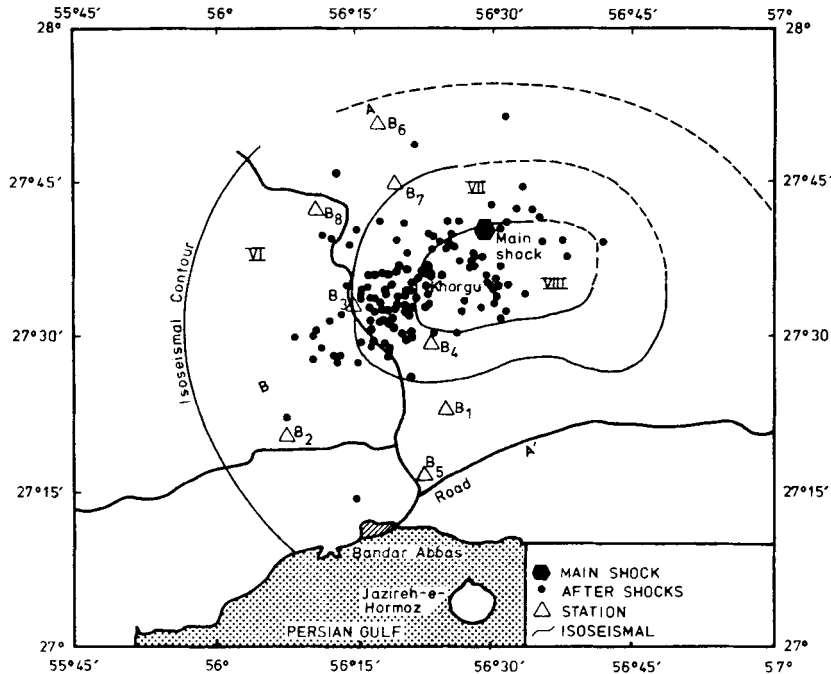

Figure 2. Location of aftershocks and isoseismal map following the Khorgu earthquake of 1977 March 21. This event did not produce observable surface displacement. The area of aftershock activities covers a broad zone of 20 km×50 km; the longer side has a trend of N50°E.
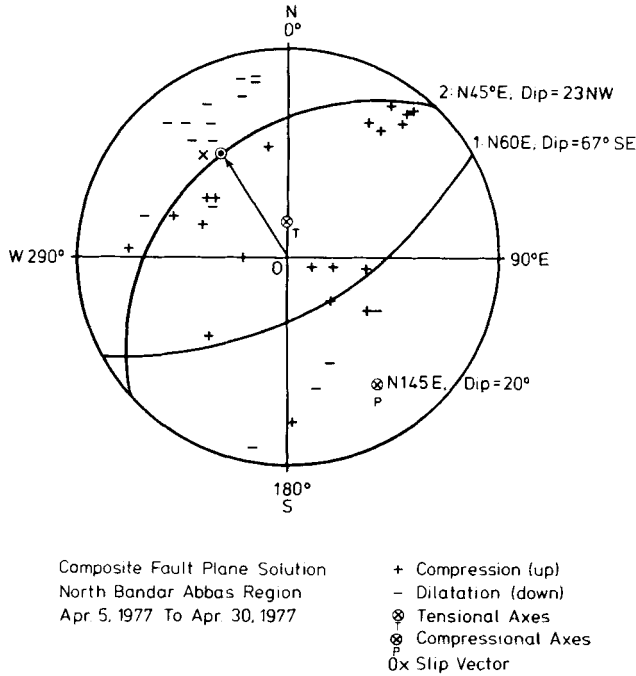
Composite Fault Plane Solution   + Compression (up)
North Bandar Abbas Region   − Dilatation (down)
Apr 5, 1977 To Apr 30, 1977   ⊗ Tensional Axes
                                  ⊗ Compressional Axes
                                  P
                                  Ox Slip Vector

Figure 3. Composite fault plane solution of the Khorgu earthquake. The slip vector, OX, is nearly perpendicular to the fold axis in the epicentral area. The compression axis is shallow and 35° east of south, indicating the general northward motion of the Arabian plate with respect to the Iranian land mass.

distribution following this event. As a result of this earthquake about 150 people were killed, over 550 suffered injuries, and more than 1500 houses were totally damaged.

Five seismographic stations were deployed following the shock. A seven-layer crustal model was used for locating the events; the details are given in a technical report by Nowroozi *et al.* (1977). The locations of over 160 relatively well-recorded aftershocks as well as the iso-seismal map for the main shock are given in Fig. 2. The majority of reported events have less than 7 km of errors in their positions. The area of the aftershock activities covers a broad area of about 20×50 km trending N50°E.
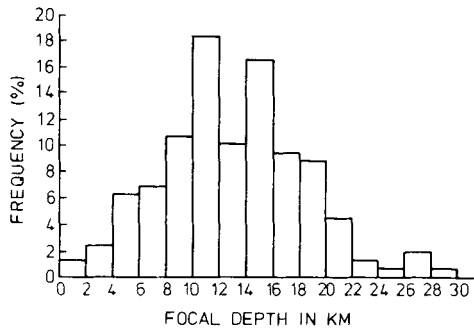
Depth Frequency Histogram Of Khorgu Aftershocks

Figure 4. Distribution of focal depths following the Khorgu earthquake. Note that the majority of events have focal depths less than 20 km.

Seismicity of Kerman Region 1900-1981
A.A. Nowroozi

LEGEND

——— Major Fault

——— Minor Fault

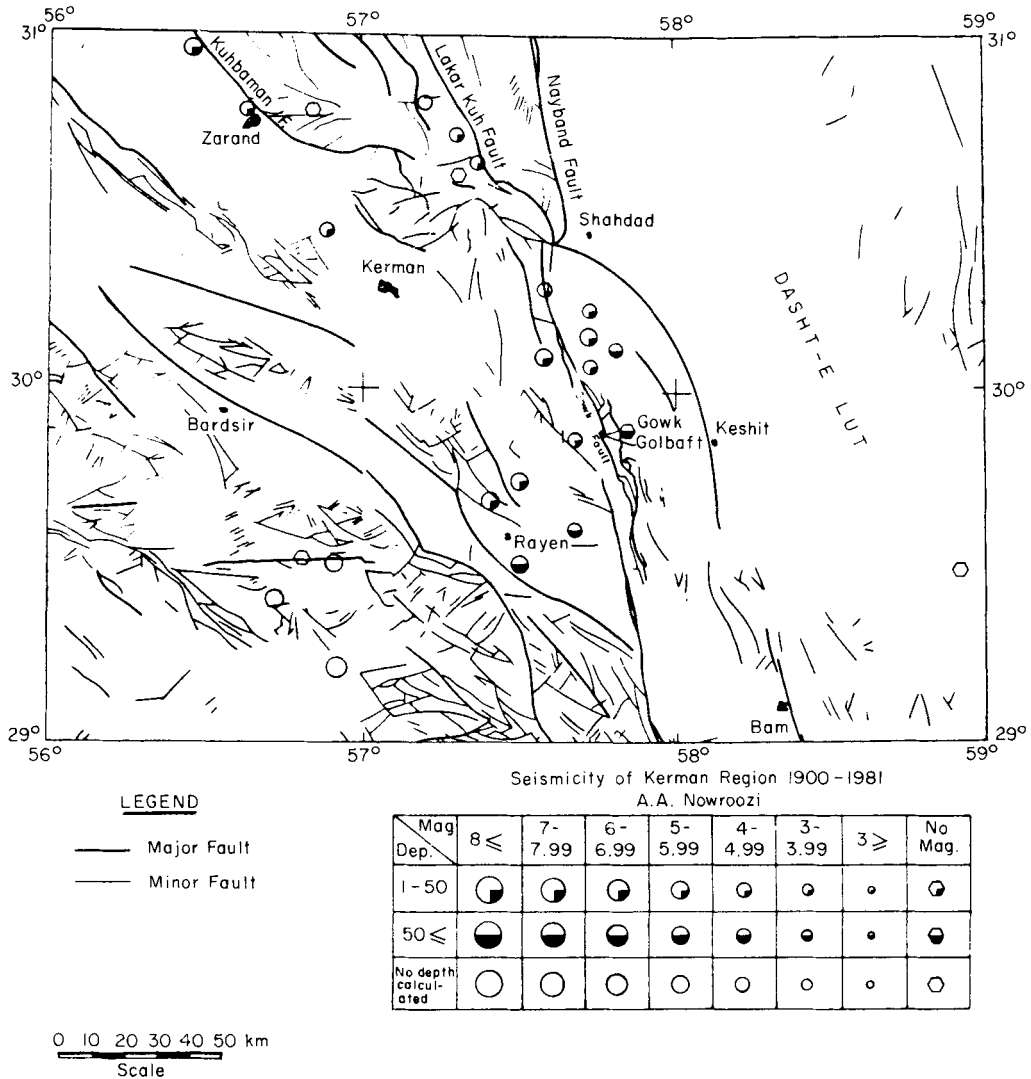| Mag. Dep.	8 ≤	7- 7.99	6- 6.99	5- 5.99	4- 4.99	3- 3.99	3 ≥	No Mag.
1-50	◖	◖	◖	◖	◖	◖	∘	◖
50 ≤	◒	◒	◒	◒	●	●	∘	◒
No depth calcul- ated	◯	◯	◯	◯	∘	∘	∘	◯

0 10 20 30 40 50 km
Scale

Figure 5. Background seismicity of the Kerman region. The Kuhbanan, Lakar-Kuh and Gowk faults are seismogenic with crustal seismicity, but in the vicinity of Rayen there are subcrustal earthquakes.

The composite fault plane solution for a number of aftershocks is given in Fig. 3 which shows nearly pure thrust faulting. The first nodal plane strikes N60°E and dips 67°SE, while the second nodal plane strikes N45°E and dips 23°NW. The compression axis strikes N145°E and dips 20°SE. Focal mechanism solutions of the Khorgu main shock and a few aftershocks are also reported by Jackson & Fitch (1981). They reported pure thrust faulting as well.

Jackson & Fitch (1981) used modelling techniques and long-period teleseismic body waves of the main shocks and a few aftershocks to determine focal depths, and concluded that the focal depths vary between 8 and 15 km. In Fig. 4, the focal depth of the aftershock series is presented. Seventy-seven per cent of the events have a depth of 8–20 km, and only about 10 per cent of the aftershocks have depths greater than 20 km; considering the uncertainties in focal depths which vary from 2 to 7 km our results are in agreement with those reported by Jackson & Fitch (1981).
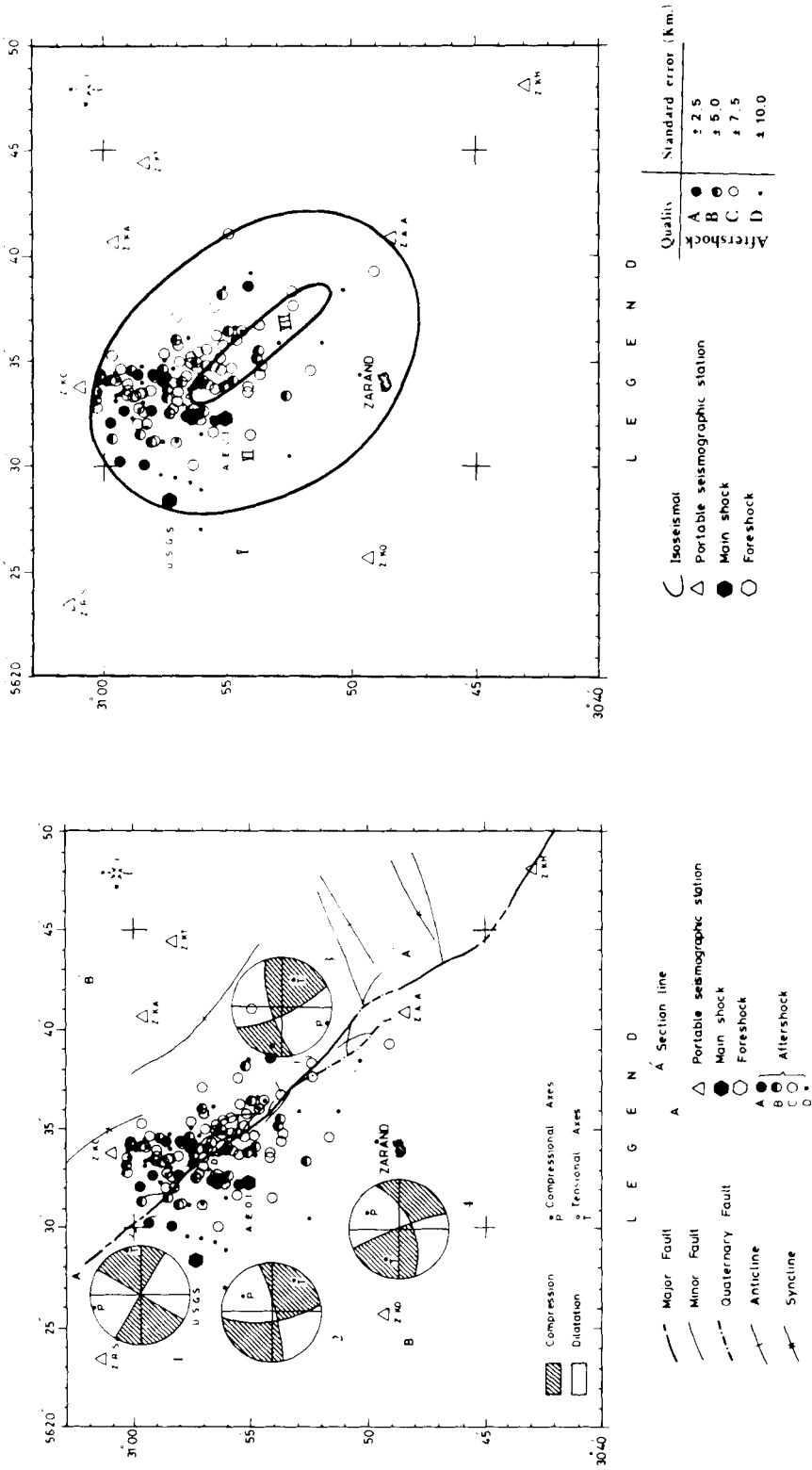
Figure 6. Aftershock activities following the Zarand earthquakes of 1977 December 19. The composite fault plane solutions indicate a right-lateral displacement in agreement with field observations (after Zohoorian *et al.* 1980).

The shallower aftershocks have a depth of about 2 km, thus it is not surprising that although the area was thoroughly searched for surface faulting, the causative fault was not found, but extensive mass wasting and areas with heavy rock falls were observed north of Bandar-e-Abbas.

The strike lines of the folded series in the vicinity of the Khorgu epicentre are N60°–N70°E, the direction of the slip vector, N30°W, obtained from the fault plane solution is nearly perpendicular to the direction of fold axis. The thrusting mechanism of this event and the direction of the slip vector indicate the northward motion of the Arabian plate relative to the Iranian land mass. This event appears to have started the increase in seismic activity in eastern Iran where six destructive earthquakes occurred which are associated with extensive faulting around the Lut plate.

The Zarand earthquake of 1977 December 19

The Zarand earthquake, M_s=5.8, occurred at 03:34:26 local time, about 70 km NW of Kerman on the Kuhbanan faults. Fig. 5 indicates major faults and prior seismicity of this region. The area between Kerman and Shahdad is very complicated structurally, as several faults meet in this locality. The background seismicity indicates that since 1900, the Kuhbanan, Lakar-Kuh, and Gowk faults have been seismically active. However, there are five events which are not readily associated with a particular fault; one event is north-west of Kerman, and four events are in the vicinity of the Rayen village. This area has a few subcrustal earthquakes as well. The event of 1979 November 9, had a depth of 119 km, when 86 stations were used for its relocation (Nowroozi 1976). Jackson & McKenzie (1984) gave a focal depth of 106 km for this earthquake while Jackson (1980) reported a depth of 114±3 km for the same event. However, the majority of the earthquakes are indeed shallow as indicated by surface faulting following the Behabad earthquakes of 1933 November 28, and the focal depths of the aftershock series following the Zarad earthquake.

Zohoorian *et al.* (1981) stated that this event killed over 500 people and injured more than 200. The damaged area is about 45×70 km. The maximum observed intensity of VIII occurred near and along the Kuhbanan fault. Fig. 6 gives the distribution of aftershocks, the isoseismal map, and the composite fault plane solutions for four segments of the Kuhbanan fault. The aftershock locations cover a triangular area on both sides of the fault, where intensity is about VI on the MM scale. The composite focal mechanism solutions indicate nearly a pure strike-slip motion. The nodal planes which are parallel to the trend of the Kuhbanan fault are taken as fault planes, thus the motions associated with the fault segments are right-lateral. The focal mechanism solutions of the main shock were deduced from teleseismic *P*-waves by Jackson & McKenzie (1984) and Berberian, Asudeh & Arshadi (1979). Their solution is in agreement with solutions presented in Fig. 6.

Berberian *et al.* (1979) reported 19.5 km of fault break at the surface with a maximum of 0.2 m right-lateral strike-slip movement along an Early Quaternary fault following this event, while Ambraseys & Melville (1982) reported a fault break of 5 km and a right lateral displacement of 50 cm following the Bahabad earthquake of 1933 November 28, M_s=6 1/4 on the same fault. The sense of movement obtained from composite solutions, as well as the main shock, are in agreement with the field evidence. The focal depths of the aftershock series indicate that more than 50 per cent of them are shallower than 16 km. The deepest aftershock had a depth of up to 26±7 km.

The Tabas earthquake of 1978 September 16

The Tabas earthquake, M_s=7.7, is the largest shock which has yet occurred within the Iranian land mass. It is located on the western border of the Lut plate. More than 19 000 persons were

killed and the entire city of Tabas was destroyed during the earthquake. Due to its size, this earthquake was studied by several different groups of workers, e.g. Mohajer-Ashjai & Nowroozi (1979), Nowroozi, Payman & Taghi-Zadeh (1980), Berberian (1979), Berberian (1982a) and Niazi & Kanamori (1981). Some disagreement exists about the extent of the faulting and displacement associated with this event (Berberian 1982b and Mohajer-Ashjai & Nowroozi 1983). Our field observation (Nowroozi *et al.* 1980) indicates that at least 75 km of fresh discontinuous thrust surface faulting, together with several branches of secondary faulting and fractures, are associated with this earthquake while the maximum vertical displacement is about 0.35 m. Berberian (1979), however, has reported 85 km of fault trace with a throw of 1.5 m and a slip of 3 m.

Focal mechanical solutions from teleseismic *P*-waves were reported by Berberian (1979) and from surface waves by Niazi & Kanamori (1981). In addition, Berberian (1982b) has given focal mechanism solutions for a number of aftershocks. The various mechanism solutions indicate a NW, SE-trending fault plane dipping towards the east. Our composite fault plane solution (Nowroozi *et al.* 1980) also indicates similar feature and is in agreement with field observations of shallow angle thrust fault (Fig. 10).

The Kurizan earthquake of 1979 November 14 and the Koli earthquake of 1979 November 27

These two destructive earthquakes occurred on the north-eastern edges of the Lut plate (Fig. 1) and produced extensive surface faulting which was mapped; a network of seismographic stations was set up for measurements of aftershock activities following the first event. Some preliminary results of field investigation were presented by Haghipour & Amidi (1980), and Nowroozi & Mohajer-Ashjai (1980) and in a report published by the AEOI (Mohajar-Ashjai *et al.* 1981). The Kurizan earthquake, $M_s=6.6$, produced a maximum intensity of VII on the MM scale in the vicinity of the village of Kurizan; as a result of this event about 200 people were killed and more than 50 were injured. The surface faulting following both earthquakes is given in Fig. 7. The Kurizan earthquake is associated with 17 km of fresh fault trace, a maximum dextral displacement of 0.9 m, and a maximum vertical displacement of 0.6 m (Fig. 11). From field investigation a macroseismic position, where maximum displacement was seen, can be adopted. This position is: lat.=33.87°N, long.=59.83°E. The fault break started south of the village of Kurizan and extended north to about 5 km east of the village of Amir Abad. Fig. 12 is a vertical view of the Kurizan fault in a valley about 5 km south of Kurizan where displacements were measured on the edges of river deposits and on the boundary of land parcels. It appears that this earthquake did not produce high ground acceleration, as the sun-dried brick adobe structures seen in Fig. 11, about 100 m from the fault trace, maintained their integrity, and their roofs did not collapse.

The Koli earthquake, $M_s=7.1$, produced a maximum intensity of at least X near the village of Koli where the maximum left-lateral horizontal displacement of 2.55 m was observed (Fig. 13). The vertical displacement at this location is 1.90 m, however, the maximum vertical displacement of 3.90 m was observed about 1.5 km west of Koli along an auxiliary branch of this fault (Fig. 14). The mapped extent of the fault is given in Fig. 7. The length of its break is at least 65 km, and it strikes nearly E–W. The 'V' shape segment of the fault trace in Fig. 7 was produced entirely after the occurrence of the Koli earthquake. The westward extension of this fault was broken following the Dast-e-Bayaz earthquake of 1968 August 31 where a maximum horizontal displacement of 5.10 m was reported by Ambraseys & Melville (1982). The new fault breakage overlaps the one associated with the 1968 earthquakes by about 20 km and extends eastward to the vicinity of Buni Aban (Fig. 8). The vertical and horizontal displacements along the fault break east of the village of Koli are given in Fig. 9. The vertical displacement appears to behave as a damped cosine
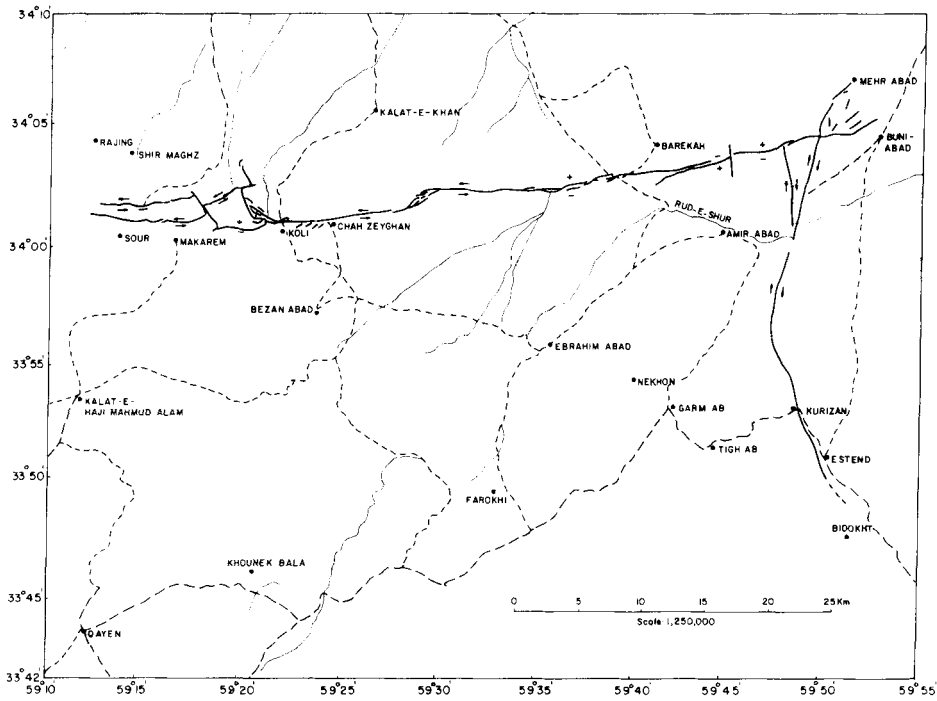
Figure 7. Earthquake faults following the Kurizan earthquakes of 1979 November 14, and the Koli earthquake of 1979 November 27. The nearly N–S fault trace from south of Amir Abad is associated with the Kurizan event; the fault length is about 17 km. Its sense of motion is right-lateral. The nearly E–W-trending fault trace from Sour to Buni Abad with several associated branches is associated with the Koli earthquake; the fault length is about 65 km. The sense of motion is left-lateral with a considerable component of complex vertical movements.
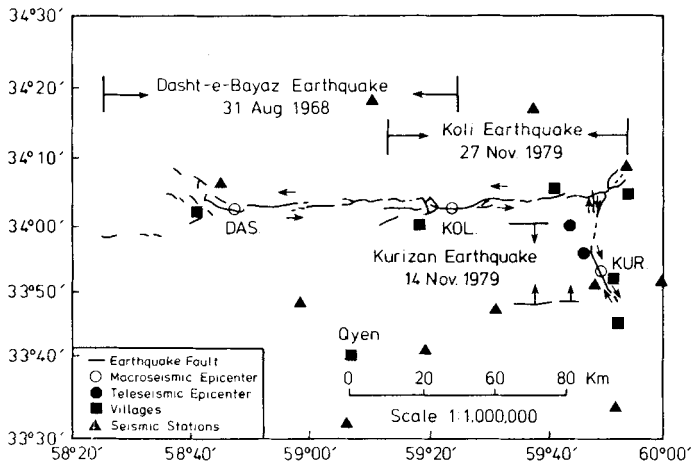

Figure 8. The fault breaks associated with the Dasht-e-Bayaz earthquake, the Koli earthquakes and the Kurizan earthquake, together with the macroseismic and instrumental epicentres. The fault associated with the Koli earthquake starts about 20 km east of the most westward end of the fault break associated with the Dasht-e-Bayaz earthquakes.
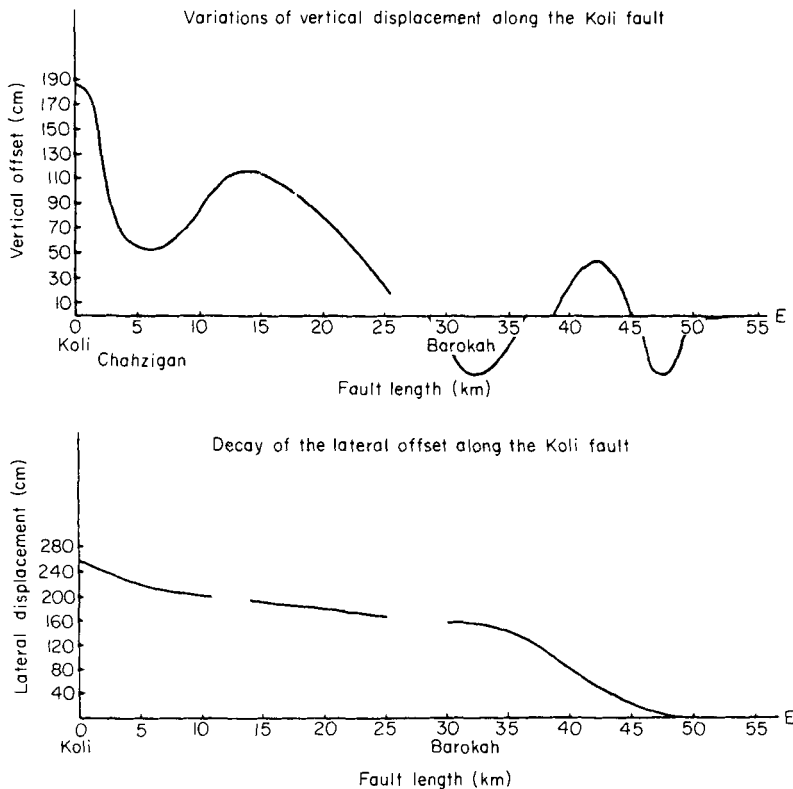
Figure 9. The variation of vertical components, upper section and horizontal component, lower section, of ground displacement along the fault trace east of Koli.

wave. Mostly, the northern block has gone up relative to the southern block. About 50 km east of Koli, vertical and horizontal displacements have damped out and are negligible.

The earthquake has produced extensive sand blows in dried river banks, where the water-table is relatively high and sands are fine and clay-free (Fig. 15). Extensive cracks and fissures accompanied by pressure ridges were observed in the vicinity of the fault breakage, thus indicating a continuous left lateral motion (Fig. 16). The striations on fault surface at Koli where maximum horizontal displacement was observed indicate that the southern block has moved down and eastward. The slip vector dips 40°–45° toward the east on a near vertical plane.

Aftershocks of the Kurizan and the Koli earthquakes

Four days after the occurrence of the Kurizan earthquake, a network of seven seismographic stations was deployed in the area. When the Koli earthquake occurred, this network was upgraded to 11 stations. Fig. 8 indicates the positions of various stations and the fault breakage. In about a month more than 2000 aftershocks were recorded. The locations of about 1000 events are given in Report 122 of the AEOI (Mohajer-Ashjai *et al.* 1981). Locations of aftershocks following the Kurizan earthquake, top section, and locations of aftershocks following the Koli earthquake, middle section, and locations of the aftershocks following both events, bottom section, are presented in Fig. 19. The locations are distributed on both sides of the fault breakage. The teleseismic location of the Kurizan event is very close to the fault breakage following this event and lies nearly at the middle of the aftershock zone.

Figure 10. The nearly N–S-trending Quaternary Tabas thrust fault about 5 km SE of Tabas; fault plane dips about 35° toward west. The surface fault trace leading to this locality had a maximum vertical displacement of about 0.35 m.

Figure 11. A 0.9 m right-lateral displacement following the Kurizan earthquake. The displacement is measured from boundaries of land parcels. Note that the adobe building about 100 m from the fault trace which is nearly parallel to the wall did not collapse. This indicates that ground acceleration produced by this event is not very high.

Figure 12. The N–S-trending Kurizan fault trace on the surface leads to a nearly E–W-trending valley about 15 km south of Kurizan village where a vertical cross-section of the fault can be seen. The fault plane is dipping toward the west near the surface, but it becomes vertical then bends toward the east in a vertical distance of less than 10 m. The fault plane is the contact between a conglomerate unit and volcanic rocks of probably Eocene age.

Figure 13. Left-lateral displacement following the Koli earthquake about 0.25 km north of Koli. The displacement is between two men standing on the hanging wall. This is about 2.55 m, while the vertical displacement in this locality is about 1.8 cm.
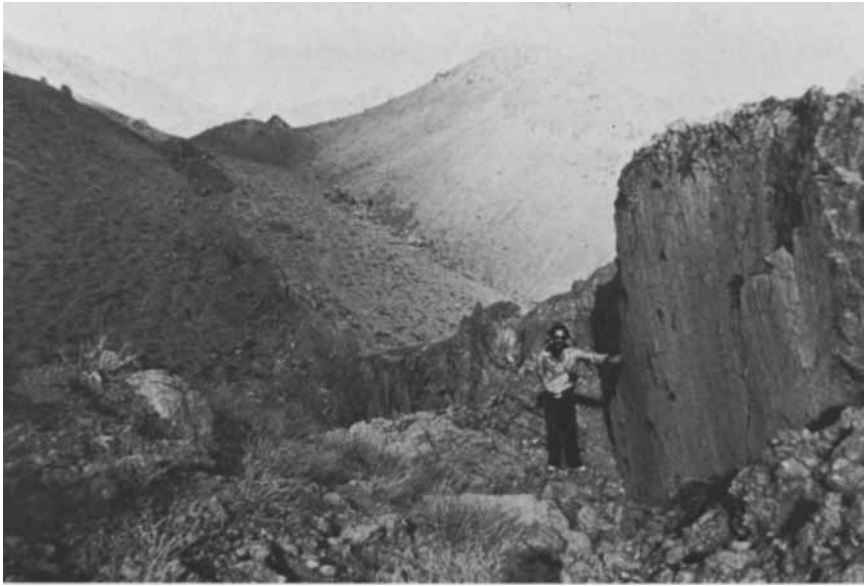
Figure 14. Maximum vertical displacement west of Koli where the displacement of 3.9 m was seen. The fault trace starts from the lower right corner and extends eastward to the upper left corner.

Figure 15. Sand blows near dried Rud-E-Shur. Many such features were seen in locations that had relatively high water-tables and well-sorted sands.

Figure 16. *En échelon* shear fracture about 20 m from the fault trace near Chah-Zeghan indicating right-lateral displacement, the direction of the hammer is E–W.

Figure 17. Vertical ground displacement on the Gowk fault. The trend of fault trace is NW/SE, the eastern side has moved upward with respect to the western side about 0.1 m.

Figure 18. Twenty centimetres right-lateral displacement on the Lakar-Kuh fault following the Chaharfarsang-Sirch earthquake.
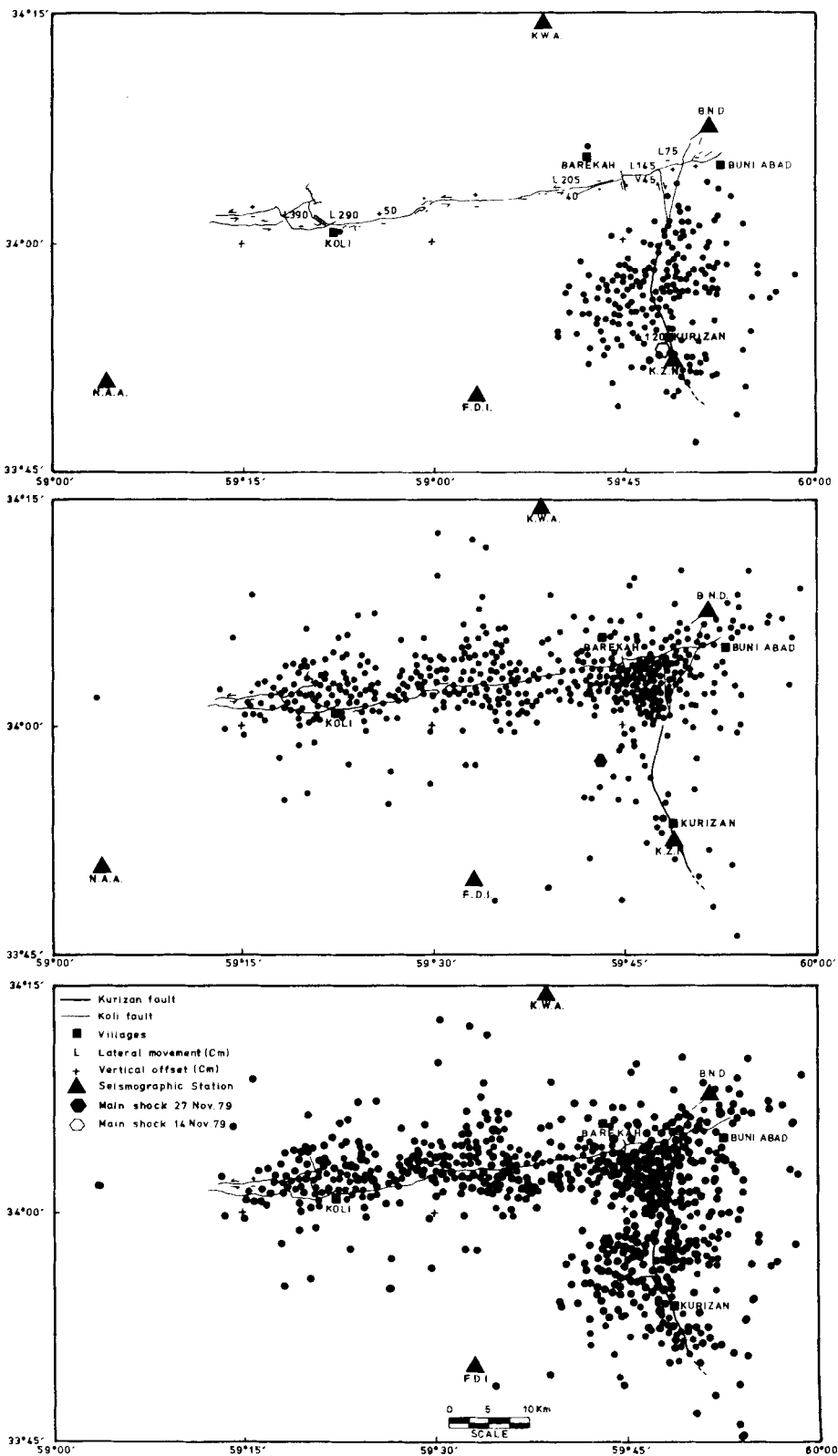
Figure 19. Aftershocks following the Kurizan earthquakes, upper section; the Koli earthquakes, middle section; and both earthquakes, lower section.
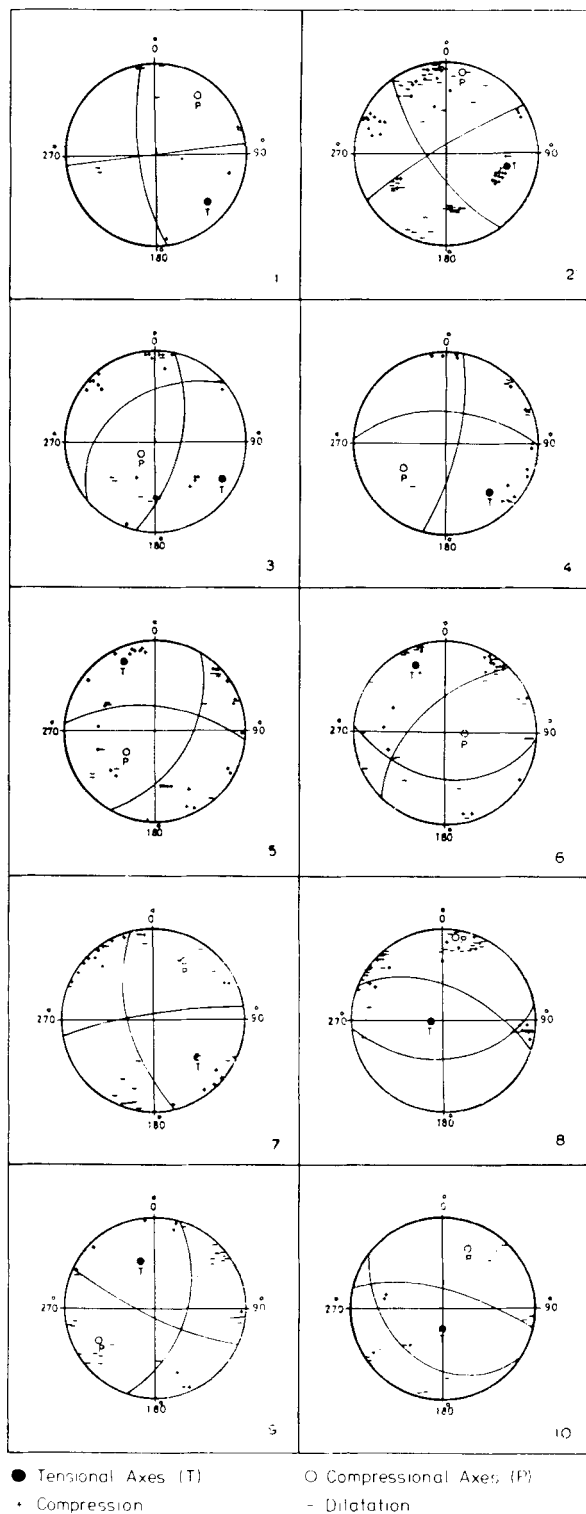
8

Figure 20. Composite fault plane solutions for 10 groups of well-recorded aftershocks. Solutions 1 and 2 are related to the two groups associated with the Kurizan fault. They show a right-lateral motion. The remaining eight solutions are related to groups associated with the Koli fault.

The teleseimic location of the Koli event is about 10 km south of the village of Bar-e-Kah near the eastern end of the Koli fault. The macroseismic location where the maximum horizontal and vertical displacements were observed is given as lat.=34.02°N, long.=59.33°E. This position is about 32 km NW of the teleseismic locations. Focal depths of the aftershock sequences of both events are shallow. Most of the events have focal depths of less than 6 km, and less than 1 per cent of the aftershocks have depths of up to 30 km. Concentration of the aftershock activities are near Buni-Abad where the N–S-trending, right-lateral Kurizan fault approaches the E–W-trending left-lateral Koli fault. This is an area where a concentration of stress is anticipated, because the rupture propagation of both faults terminated at this point, thus the aftershock activities are pronounced.

Composite fault plane solutions of a number of well-determined aftershocks following the Kurizan earthquake are given in Fig. 20. The Kurizan fault is divided into two segments. The composite solutions for each segment are given in Fig. 21 next to each fault segments. Both solutions indicate a right-lateral motion as expected from the field observation. Jackson & McKenzie (1984) have given the teleseismic fault plane solution of the main shock. Their solution is in agreement with our composite solutions of the first segment where the fault plane is rather steep and its trend is nearly N–S. Field observation (Fig. 12), indicates that the fault plane dips west near the surface; however, in a vertical distance of about 5 m down, the fault plane changes to near vertical and then bends over towards the east. Variation of the dip angle with depth may be the cause of dispersion of the aftershock locations as indicated in Fig. 20.

The Koli faults are broken into eight segments. The composite solutions for each segments are given individually in Fig. 20 and next to the fault segments in Fig. 21. Segment number 3 has a 'V' shape. The right edge of the V appears to be a continuation of the Kurizan fault, and the left edge of the V is nearly perpendicular to the Koli fault trace. These segments were carefully checked in the field; both parts have occurred after the Koli earthquakes. The sense of motion for the V
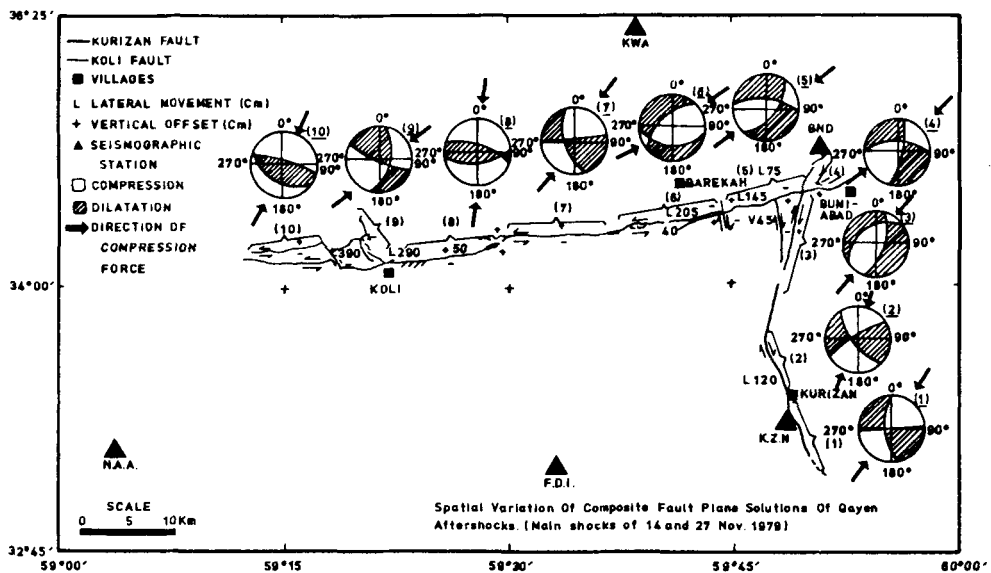
Figure 21. Composite fault plane solutions corresponding to aftershocks associated with each fault segment. Solutions 1 and 2 are related to the Kurizan fault and indicate right-lateral motion. Solution 2, 5 and 6 are related to branches of the Koli fault and indicate a normal component; solutions 8 and 10 indicate a thrust component; and solutions 4, 5, 7 and 9 indicate left-lateral motion. The Koli fault is a multiple event with very complex faulting.

shape branches of this fault are both right-lateral and in agreement with the sense of motion of the Kurizan fault. However, a substantial amount of vertical motion was observed where the middle part of the 'V'-shaped block had moved down relative to its right edge. The mechanism solution indicates a small right-lateral component of movement along the N–S-trending nodal plane, but predominant motion on this segment is normal faulting which is in agreement with field observation. We believe this segment, which appears as a continuation of the Kurizan fault, is activated by the occurrence of the Koli earthquake.

Segment number 4 tends nearly E–W. The mechanism solution indicates a left-lateral motion as expected. The fault plane dips about 60° toward the north, segment numbers 4, 5, 7 and 9 also show left-lateral motion along an E–W trending nodal plane. Segment number 6, near the village of Bar-e-Kah, has a substantial amount of normal component. At this area a small N–S trending fault was detected on the ground and the northern block has moved down relative to the southern block. Segment number 7 indicates almost a pure left-lateral strike-slip on a steep, nearly E–W nodal plane. Segments 8 and 10 indicate large components of thrust mechanism on an E–W trending nodal plane. These two segments of the Koli fault are extremely complex as indicated in Fig. 21. The fault segments are not rectilinear, but splay out into several branches, thus a simple left-lateral motion on the straight segment may change into thrust motions on the splays. Some of the aftershocks of the Dasht-e-Bayaz earthquakes of 1968 August 31 also indicated a thrust mechanism (Nowroozi 1972 and Jackson & McKenzie 1984). The focal mechanisms of the main shocks for both the Kurizan and Koli earthquakes are reported by Jackson & McKenzie (1984). Their solution for the Kurizan earthquakes is in agreement with our two composite solutions for segments 1 and 2 of the Kurizan fault, and their solution for the Koli earthquake is in agreement with our composite solutions on segment numbers 4, 7 and 9. The fault breakage appears, however, to be more complicated than a simple left-lateral fault. The Koli earthquake is definitely a multiple event with complex surface faulting pattern as is indicated by its ground displacements given in Fig. 9. Field observations indicate that the vertical component of ground displacement along the western 55 km of the fault trace appears to have the form of damped oscillations, while the horizontal component dies out along the fault trace.

The Golbaf earthquake of 1981 June 11 and the Chaharfarsang-Sirch earthquake of 1981 July 28

These two destructive earthquakes occurred less than two months apart in the south-western edge of the Lut plate. Both earthquakes are on previously recognized faults; however, ground displacements were not of substantial magnitudes as is usually expected for the earthquakes in eastern Iran. Some preliminary results following these events were discussed by Mohajer-Ashjai & Nowroozi (1984), Zohoorian, Kabiri & Ghamsari (1985) and Adeli (1982), while Berberian *et al.* (1984) discussed results from their teleseismic and field data.

The Golbaf earthquake, $M_s = 6.8$, occurred at 10:56 local time about 80 km SE of Kerman. It killed nearly 1100 persons and more than 4000 were injured. The maximum intensity was about VII on the MM scale and covers an area of more than 80 square km. This event occurred in the previously recognized Gowk fault which is Quaternary in age, and it cuts through recent alluvium in the Golbaf Valley (Fig. 22), where 16 km of discontinuous surface fracture was mapped. The maximum vertical displacement was about 10 cm SE of Golbaf and east of Tirgan (Fig. 17). In this locality the fault trends N 25° W, and the eastern side has moved up relative to the western side. The movement is associated with a small right-lateral component; however, due to local slumping and rock falls, no accurate horizontal displacement was measureable. The movements on the Gowk fault have probably been the cause of earthquakes in 1946, 1948, 1969 and 1975 as well. The Gowk fault extends southwards to 29.4°N latitude and disappears in recent alluvium deposits.
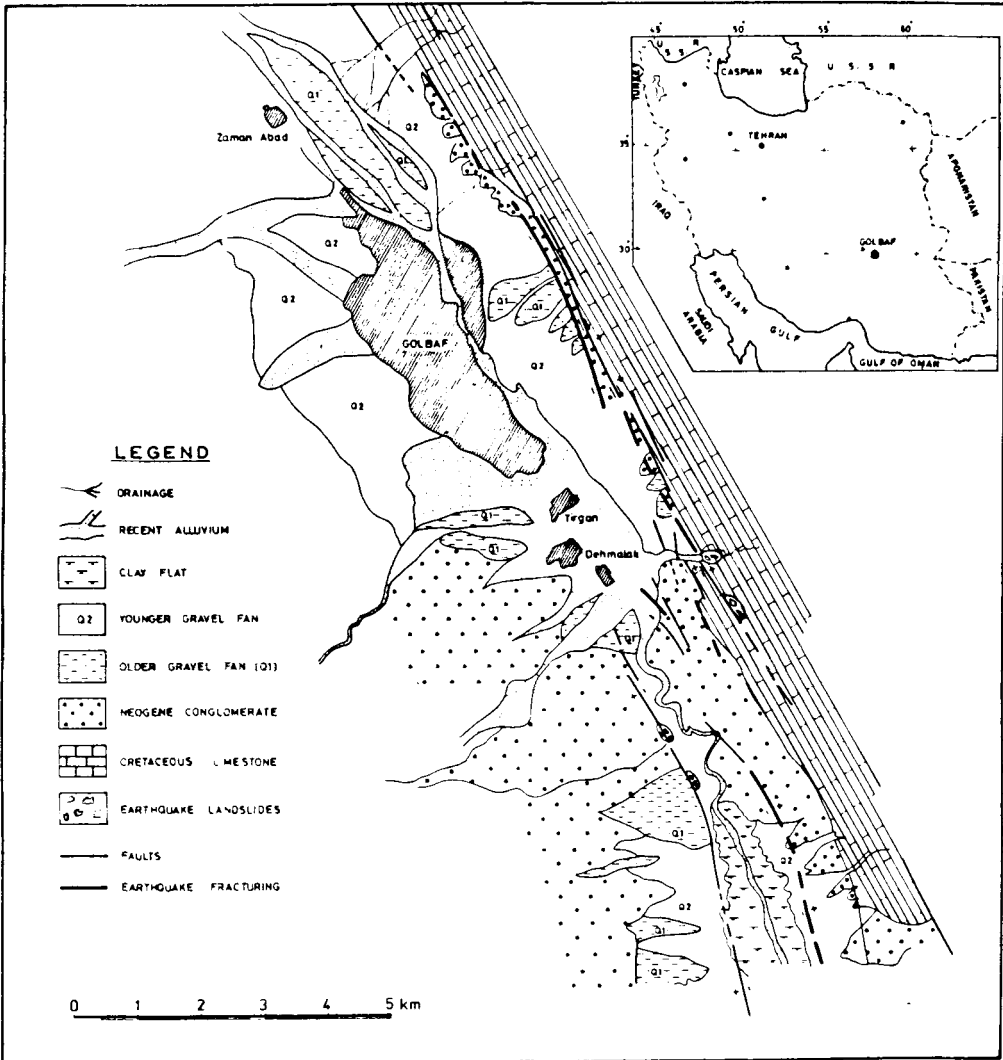
Figure 22. Earthquake fault following the Golbaf earthquake; several branches of the Gowk fault were moved after this event.

The Chaharfarsang-Sirch earthquake, M_s=7.1, occurred 47 days later. Its epicentre is about 30 km north of the Golbaf epicentre. Many people lost their homes; however, as they had moved into tents following the first earthquake, only about 400 people were killed after this event. The maximum intensity was about VII on the MM scale. The earthquake was associated with over 65 km of discontinuous surface faulting, fracture and severe mass wasting, and landslides. The fault trace associated with this earthquake is the northward continuation of the Gowk fault where a series of discontinuous branches and fractures was observed and mapped. At least two NNE branches were seen from Fandogha to the north of Sirch. These branches have the trend of the Gowk fault and the field observations indicate that the eastern block has moved up relative to the western block. Several small N–S branches which have a trend similar to the trend of the Nayband fault were also detected. Careful examination of these branches indicates that north of Chaharfarsang the trend of faulting has changed from nearly N–S to NW/SW and movement has

occurred on the previously recognized Lakar-Kuh fault. Again, the eastern block has moved upwards with respect to the western block. In the vicinity of Chaharfarsang several faults meet. These faults are Bam, Nayband, Lakar-Kuh, and Gowk. But the Chaharfarsang-Sirch earthquake is associated only with movement along the northern portion of the Gowk fault and the south-eastern end of the Lakar-Kuh fault where about 20 cm of horizontal right-lateral displacement was detected (Fig. 18). The vertical motion on this fault is about 15 cm.

The observations can be interpreted as reverse faulting with a small component of right-lateral motion. Distribution of the aftershock locations following the Golbaf earthquake is given in Fig. 23. The main fractures of the fault are well covered by the aftershocks although there are unusual number of events NE of the observed main fractures.

Zohoorian *et al.* (1985) have made an attempt to determine the fault mechanism from composite fault plane solutions. Based on their interpretation, various groups of aftershocks indicate mainly normal faulting with small components of right-lateral motion. An examination of their solutions indicate that there are many abnormal readings which may be due to complicated fault behaviour in this region as discussed by Berberian *et al.* (1984). Jackson & McKenzie (1984) gave fault plane solution for the main shock; assuming their N172°E nodal plane as the fault plane, the solution indicates thrust faulting with a right-lateral component of motion; the fault plane dips 40° toward the west. This is in agreement with the distribution of the aftershock location which indicates a NW/SE trend and its dispersion around the observed fractures. The focal depths of the events are shallow, and the majority of them have a depth of less than 15 km.

The distribution of aftershock locations following the Chaharfarsang-Sirch earthquake is given in Fig. 24. The aftershock zone is mainly west of the observed fractures with a concentration near the village of Chaharfarsang where the Lakar-Kuh, Nayband, Gowk and Bam faults meet; focal depths for these aftershocks also are mostly less than 15 km. Again, attempts to find composite fault plane solutions for various groups of earthquakes failed because of many inconsistencies due
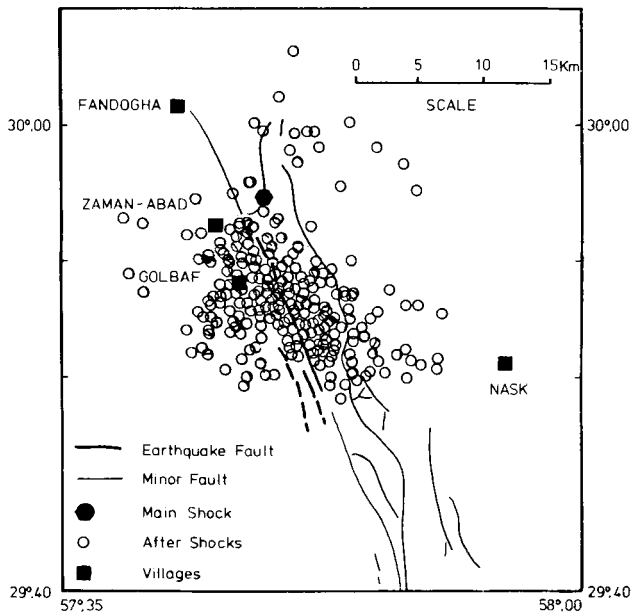

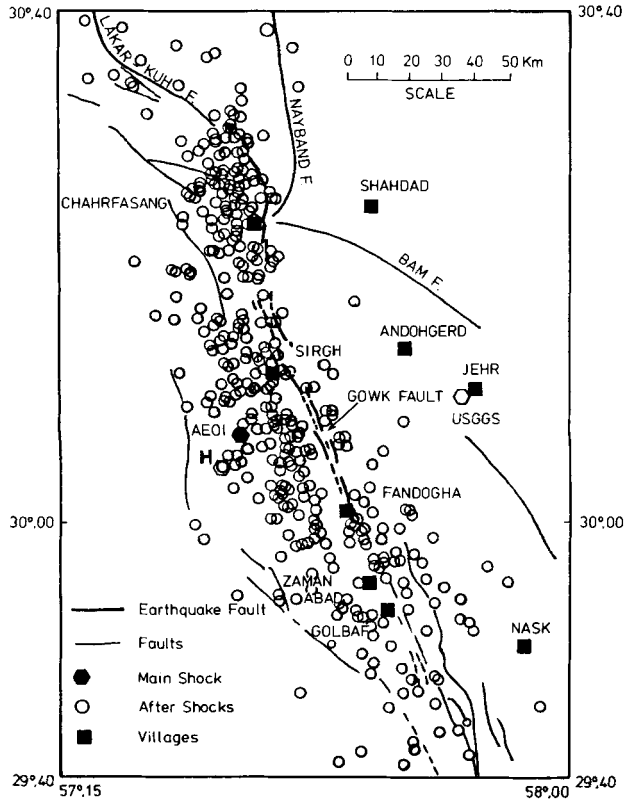**Figure 23.** Aftershock locations following the Golbaf earthquake.

Figure 24. Aftershock locations following the Chaharfarsang-Sirch earthquake. The epicentre of the main shock given by USCGS is given by open hexagonals.

to the multiple nature of the fracture pattern as discussed by Berberian *et al*. (1984). Jackson & McKenzie (1984) and Dziewonski & Woodhouse (1981) reported the source mechanism for the main shock. Both solutions indicate thrust faulting with a small component of horizontal motion. The trends of both nodal planes given by Jackson & McKenzie are similar to the trend of the Lakar-Kuh fault. In addition, the majority of the aftershocks are SW of the observed motion on this fault; thus, we interpet the N127°E nodal plane of Jackson & McKenzie as the fault plane which dips 52° toward the SW. This interpretation would indicate a small component of right-lateral motion and is in agreement with the field observation of 0.2 m right-lateral displacement on the Lakar-Kuh fault, north of Chaharfarsang (Fig. 18).

Deformation of the Lut plate boundaries

As was indicated before, except for the Khorgu earthquake which occurred in the Fars folded series of Zagros, the remaining six events occurred on the greater deformational boundaries of the Lut plate. The detailed geology of this region is not available. The result of a reconnaissance survey is discussed by Stocklin (1968). A more recent map of this region is published by Huber (1977). The major faults, volcanoes, and structural trends of south-eastern Iran, including the Lut, is proposed on Fig. 25, and the seismicity of all Iran up to 1982 is given in Fig. 26. The boundaries of Lut are relatively broad and not well established in the southern and northern portions. However, on the eastern and western regions there is more agreement among
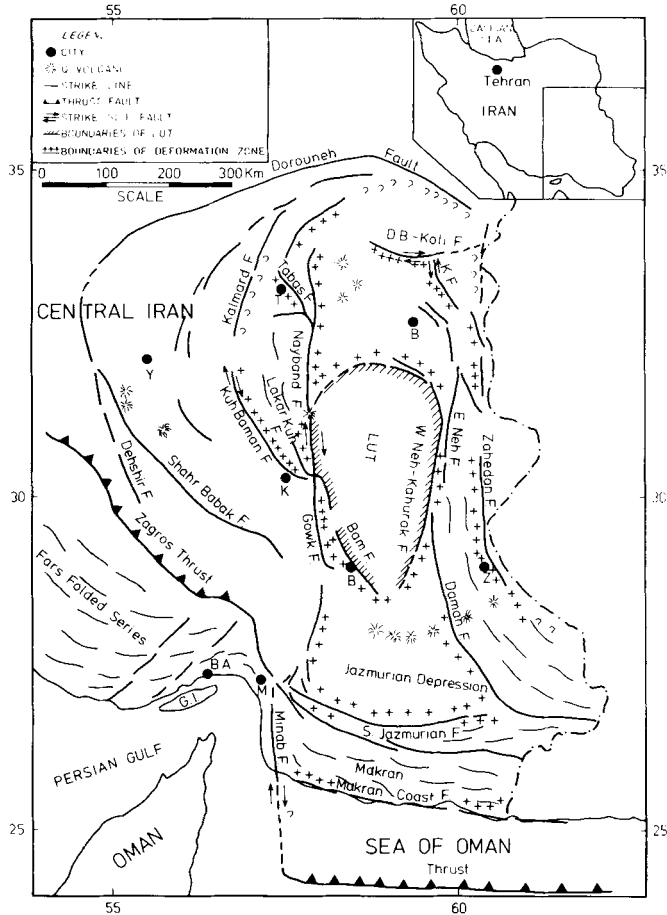
Figure 25. Proposed deformational boundary of the Lut plate.

numerous authors, and the boundaries are narrower. According to Stocklin (1968), the Lut block is irregular in shape, essentially N–S-trending, rigid mass, smoothly surrounded by the ranges of central and eastern Iran. The N–S trends in the Tabas block and the eastern Iranian ranges as well as the arcuate shape of the Dorouneh fault to the north of it are probably enforced by the shape and rigidity of the Lut block. Gansser (1969) asserted that the Lut block is a leftover of a once widely propagating median mass of Iran. The Lut itself is mostly covered by sand dunes on the east, wind-eroded loesses on the west, and flat lying Palaeogene volcanoes on the north. Seismicity within the oval shape which is the new proposed Lut plate is minor (Fig. 26). Most of the major earthquakes, as were discussed before, occur on a broad zone surrounding this median plate. Stocklin (1968) reported an extensive sub-horizontal Mesozoic sedimentary cover in the Tabas block on the western boundary of Lut, the largest earthquakes inside Iran, $M=7.7$,

Figure 26. Seismicity of Iran from 1900 to 1982. The data bases are from Nowroozi (1971, 1976), Nabavi (1977), ISS, PDE, and locations reported by the Atomic Energy Organization of Iran (AEOI) and the Institute of Geophysics of Tehran University. The faults are taken from Huber (1977), Berberian (1976), and Stocklin & Nabavi (1972). Note the effect of the Zagros thrust fault on the seismic pattern. South-west of the thrust seismicity is sheet-like and more continuous, maximum magnitude is about 7.1. There is no observed faulting associated with an earthquake in the SW seismic zone. North-west of the thrust seismicity is more sporadic, and the maximum magnitude is about 7.7. In east Iran, often earthquakes are associated with well-observed surface faulting.

occurred not too far from these sedimentary units. He also reported relatively undeformed sedimentary units in isolated places in the central Lut near 31°N, 57°E. Gansser (1969) defined the boundary of the Lut block by the Nayband fault on the west, the Dorouneh fault on the north, and a series of complicated faults and steep thrust on the east. Nowroozi (1972) used plate tectonic concepts and, influenced by the extensive displacement and faulting following the Dasht-e-Bayaz earthquake of 1968, assumed the causative Ferdows or Dasht-e-Bayaz fault as the northern boundary of the Lut plate. The same fault broke about 65 km eastward during the Koli earthquake of 1979, the total length of this fault now is about 145 km. Mohajer-Ashjai, Behzadi & Berberian (1975) used satellite imagery of eastern Iran and evaluated the recent tectonics of the Lut block. They discovered several units of arcuate structures, lineaments, and volcanic cones within the northern part of it; thus, they argued against its rigidity as proposed by Stocklin (1968). Jackson & McKenzie (1984) interpreted the entire eastern part of Iran, including the Lut block as a zone of deformation. Fig. 25 gives a new interpetation of the boundary of the Lut plate. The immediate inner boundary of Lut is clearly indicated by the seismogenic Bam and Nayband faults on the west, and the west Neh-Kahurak faults on the east. The width of these zones where deformations take place varies from a few tens to over 100 km as indicated on Fig. 25. On the west side most of the deformation takes place between the Kuhbanan and Nayband fault NE of Kerman and the Gowk and the Bam fault SE of Kerman. The Kuhbanan fault is active up to about 32°N, 56°E where the Kalmard fault starts, the latter has not shown signs of recent or historic seismicity as indicated in Fig. 26. Thus the north-western boundary of this deformation zone and its connection to the deformation zone near Tabas is questionable as indicated in the figure. The eastern deformation zone extends from the west Neh-Kahurak fault to the Zahedan fault. Stocklin (1974) extends this fault northward into the Turan platform. The width of this zone is composed of flych-type deposits and patches of coloured mélanges. The northern deformation zone of the Lut is of extensive extent where most volcanic cones and arcuate structures occur (Mohajer-Ashjai *et al.* 1975). As most seismic activity is at present associated with the Dasht-e-Bayaz-Koli fault which has been broken following the 1968 and 1979 earthquakes (Fig. 26), we interpret this fault as the northern boundary of the deformation zone, although part of Doruneh may also be another candidate. The southern extension of the Lut merges into a series of volcanic rocks and several recent to subrecent volcanic cones. Relocated epicentres indicate a few subcrustal earthquakes within this deformational zone south of the Lut plate. Jackson & McKenzie (1984) adopted depths of the 1969 November 7 and 1968 August 2 earthquakes as 74 and 62 km respectively. The relocated depths, however, are 41 km for the 1969 event and 74 km for the 1968 event (Nowroozi *et al.* 1977). The southern extension of the deformational zone includes an E–W-trending ophiolite zone along the southern limit of the Jazmurian depression which is marked by the south Jazmurian fault. However, Makran units have gone through considerable crustal shortening as displayed by progressivly younger and less deformed sedimentary units southward (Farhoudi & Karig 1977). The E–W-trending Makran ranges are composed of Palaeogene flysch type sedimentary units and patches of coloured mélanges. The Makran ranges are delineated on the west by the N–S-trending seismically active Minab fault. This active fault connects the Zagros thrust to the Sea of Oman thrust fault which is E–W-trending and occurs about 150 km south of the Makran coast (Stoneley 1974). Therefore, the Minah fault is a transform fault which connects two concave type thrusts (Wilson 1965). The convergence characteristic along the Arabian–Iranian plate boundary (see Nowroozi 1972 and Jackson & McKenzie 1984) changes severely eastward of the Minab Transform fault. To the west lies the collision and subduction of the continental crust of the Arabian plate against central Iran and to the east lies subduction of the oceanic crust under the Makran ranges. Thus, crustal shortening and thickening occurs in the sedimentary units of Zagros which is supported by many thrust-type focal mechanism solutions reported for the earthquakes in the Zagros region
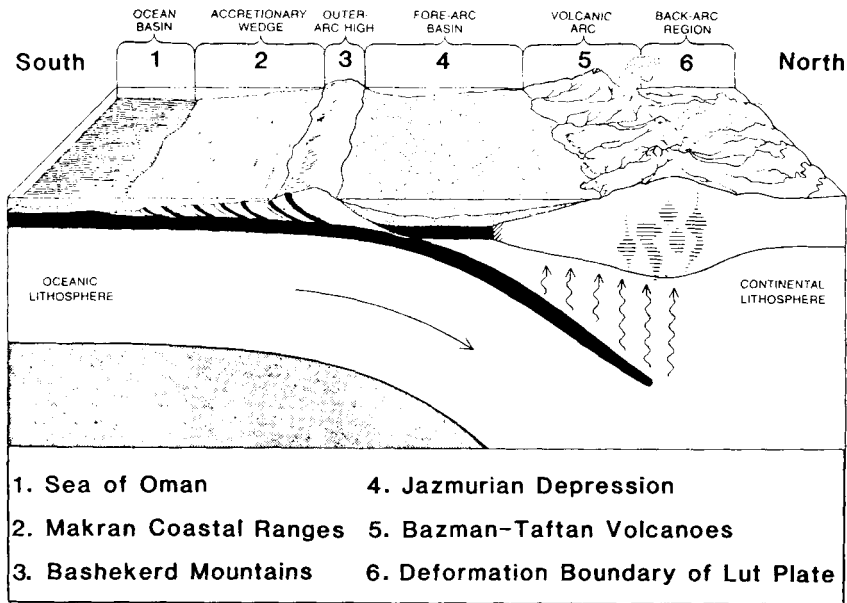
Figure 27. A hypothetical N–S cross-section across eastern Iran from the Makran coastal ranges to the southern limits of the Lut plate. The six characteristics sequence of geological features discussed by Burchfiel (1983) are identified for this active convergent plate boundary.

(Nowroozi 1972, McKenzie 1972 and Jackson & McKenzie 1984). The crustal consumption under the Makran ranges is supported by the E–W-trending uplifts along the coast, the recent to subrecent volcanic cones of the Bazman Taftan series, and a few subcrustal earthquakes (Nowroozi 1976 and Jackson & McKenzie 1984). Furthermore, many focal mechanism solutions for earthquakes in the Makran region show thrust motion along a nearly E–W-trending nodal plane, thus indicating subduction of the Arabian Sea under the Iranian coast ranges of Makran. Therefore, the Makran sedimentary unit may be another outer belt of deformational zone surrounding the southern boundary of the Lut plate.

An active arc and convergent plate boundary appears to exist from the Makran coast of Iran to the southern boundary of the Lut plate where the oceanic crust of the Arabian Sea and the Sea of Oman underthrust eastern Iran. This type of oceanic–continental collision is often marked by a characteristic sequence of geological features as recently discussed by Burchfiel (1983). The sequence consists of six units. These six distinct geological features are recognized in Fig. 27. From south to north the units are: The Sea of Oman followed by the E–W-trending Makran coastal ranges which are composed of flysch-type sediments and patches of coloured mélanges and ophiolite suites. The entire coastal ranges act as an accretionary sedimentary wedge. This is followed by the outer arc high or Bashekerd mountain chains. The Jazmurian depression forms the forearc basins where alluvium deposits are accumulated at present. Then starts the active andesitic Taftan-Bazman chain of volcanoes. The backarc region is the southern deformational boundary of the Lut plate where active faulting is in progress at present.

References

Adeli, H., 1982. The Sirch (Kerman, Iran) earthquake of 28 July 1981: a field investigation, *Bull. seism. Soc. Am.*, **82**, 841–861.

Ambraseys, N. N. & Melville, C. P., 1982. *A History of Persian Earthquakes*. Cambridge University Press.

Berberian, M., 1976. Contribution to seismotectonics of Iran, *Publs geol. Surv. Iran, No. 39.*

Berberian, M., 1979. Earthquake faulting and bedding thrusts associated with the Tabas-e-Golshan (Iran) earthquake of 16 September 1978, *Bull. seism. Soc. Am.*, **68**, 1861–1887.

Berberian, M., 1982a. Aftershock tectonics of the Tabas-e-Golshan (Iran) earthquake sequence: a documented active 'Thick and Thin Skinned Tectonics' case, *Geophys. J. R. astr. Soc.*, **68**, 499–530.

Berberian, M., 1982b. Discussion on the paper, A. Mohajer and A. A. Nowroozi, The Tabas earthquake of Sept. 16, 1975, in East-central Iran, *Geophys. Res. Lett.*, **9**, 193–194.

Berberian, M., Asudeh, I. & Arshadii, S., 1979. Surface rupture and mechanism of the Boh-Tangol (south-eastern Iran) earthquake of 19 December 1977, *Earth planet. Sci. Lett.*, **42**, 456–462.

Berberian, M., Jackson, J. A., Ghorashi, M. & Kadjar, M. H., 1984. Fields and teleseismic observations of the 1981 Golbaf-Sirch earthquakes in SE Iran, *Geophys. J. R. astr. Soc.*, **77**, 809–838.

Berberian, M. & Papastamatiou, D., 1978. Khorgu (North Bandar Abbas, Iran) Earthquake of March 21, 1977: a preliminary field report and seismotectonic discussion, *Bull. seism. Soc. Am.*, **68**, 411–428.

Burchfiel, B. C., 1983. The continental crust, *Sci. Am.*, **249**, 130–146.

Dziewonski, A. M. & Woodhouse, J. H., 1981. *PDE*, National Earthquakes Information Service, United States Geological Survey.

Farhoudi, G. & Karig, D., 1977. Makran of Iran and Pakistan as an active arc system, *Geology*, **5**, 664–668.

Gansser, A., 1969. The large earthquakes in Iran and their geological frame, *Eclog. geol. Helv.*, **62**, 443–466.

Haghipour, A. & Amidi, M., 1980. The November 14 to December 25, 1979 Ghaenat earthquakes of Northeast Iran and their tectonic implications, *Bull. seism. Soc. Am.*, **70**, 1751–1757.

Huber, H., 1977. *Geological Map of Iran*, scale 1:1,000,000, National Iranian Oil Company.

Jackson, J. A., 1980. Errors in focal depth determination and the depth of seismicity in Iran and Turkey, *Geophys. J. R. astr. Soc.*, **61**, 285–301.

Jackson, J. A. & Fitch, T. J., 1981. Basement faulting and the focal depths of the larger earthquakes in the Zagros mountains (Iran), *Geophys. J. R. astr. Soc.*, **64**, 561–586.

Jackson, J. A. & McKenzie, D., 1984. Active tectonics of Alpine-Himalayan Belt between western Turkey and Pakistan, *Geophys. J. R. astr. Soc.*, **77**, 185–264.

Lahr, H. & Ward, P., 1973. Hypoellipse computer program, *Open File Rep. U.S. geol. Surv.*

McKenzie, D. P., 1972. Active tectonics of the Mediterranean region, *Geophys. J. R. astr. Soc.*, **30**, 109–185.

Mohajer-Ashjai, A., Behzadi, H. & Berberian, M., 1975. Reflection on the rigidity of the Lut Block and recent crustal deformation in eastern Iran, *Tectonophys.*, **25**, 281–301.

Mohajer-Ashjai, A. & Nowroozi, A. A., 1979. The Tabas earthquake of Sept. 16, 1975, in East Central Iran, *Geophys. Res. Lett.*, **9** (3), 193–194.

Mohajer-Ashjai, A. & Nowroozi, A. A., 1983. Reply to Berberian's comments on the paper, A. A. Mohajer-Ashjai and A. A. Nowroozi, Tabas earthquake of Sept. 16, 1978 in east central Iran, G.R.L. 9L0391, *Geophys. Res. Lett.*, **10** (3), 199–202.

Mohajer-Ashjai, A. & Nowroozi, A. A., 1984. Damage distribution and aftershock of two major events of 1981 in Kerman region SE Iran, *Abstr. 27th int. Geological Congress*, Moscow, July.

Mohajer-Ashjai, A., Nowroozi, A. A., Taghi-Zadeh, G. & Zohoorian, A. A., 1981. A report on two earthquakes in Ghaenat (Iran): aftershocks, faultings, and damages, *Techn. Rep. 122*, Atomic Energy Organization of Iran (in Farsi).

Nabavi, M. S., 1977. Aspects of the seismic behaviour of Iran, especially the southern Zagros area, *PhD thesis*, University of London.

Niazi, M. & Kanamori, H., 1981. Source parameters of the 1978 Tabas and 1979 Quinat, Iran earthquakes from long period surface waves, *Bull. seism. Soc. Am.*, **71**, 1201–1213.

Nowroozi, A. A., 1971. Seismotectonics of the Persian plateau, eastern Turkey, Caucusus and Hindu-Kush region, *Bull. seism. Soc. Am.*, **61**, 317–341.

Nowroozi, A. A., 1972. Focal mechanism of earthquakes in Persia, Turkey, West Pakistan, and Afghanistan and plate tectonics of the Middle East, *Bull. seism. Soc. Am.*, **62**, 832–850.

Nowroozi, A. A., 1976. Seismotectonic provinces of Iran, *Bull. seism. Soc. Am.*, **66**, 1249–1276.

Nowroozi, A. A. & Mohajer-Ashjai, A., 1980. Faulting of Kurizan and Koli (Ghaenat, Iran) earthquakes of November 1979: a field report, *Bull. Bur. Mech. Géol. Min.* (Dauxiene series), sect. IV, **2**, 1980/1981, 90–98.

Nowroozi, A. A., Mohajer-Ashjai, A., Rad, E. & Zohoorian, A. A., 1977. *The main shock and aftershocks of the March 21, 1977 earthquake in the Khorgu region, Techn. Rep.*, Atomic Energy Organization of Iran.

Nowroozi, A. A., Payman, M. & Taghi-Zadeh, 1980. Aftershock sequence and field report on the major Tabas earthquake in East-Central Iran, *Bull. Iranian Petrol. Inst.*, **77**, 15–30 (in Farsi).

Shoja-Taheri, J. & Niazi, M., 1981. Seismicity of the Iranian Plateau and Bordering regions, *Bull. seism. Soc. Am.*, **71**, 477–489.

Stocklin, J., 1968. Structural history and tectonics of Iran – a review, *Bull. Am. Ass. Petrol. geol.*, **52**, 1229–1258.
Stocklin, J., 1974. Possible ancient continental margins in Iran, in *The Geology of Continental Margins*, pp. 873–887, eds Burke, C. A. & Drake, C. L., Springer-Verlag, New York.
Stocklin, J. & Nabavi, M. H., 1972. *Tectonic Map of Iran*, scale 1:2,500,000, Geological Survey of Iran.
Stoneley, R., 1974. Evolution of the continental margin bounding a former southern Tethys, in *The Geology of Continental Margins*, pp. 889–903, eds Burke, C. A. & Drake, C. L., Springer-Verlag, New York.
Wilson, J. T., 1965. A new class of faults and their bearing on continental drift, *Nature*, **207**, 343–347.
Zoohorian, A. A., Kabiri, A. & Ghamsari, M., 1985. Distribution of damages and aftershock activities of two major 1979 earthquakes in east of Kerman, Iran, *J. Earth Space Sci.*, submitted, Tehran University Press (in Farsi).
Zohoorian, A. A., Mohajer-Ashjai, A., Salehi, M. R. & Taghizadeh, G. A., 1981. *J. Earth Space Sci.*, **1, 2**, 25–42, Tehran University Press.